A Theoretical Analysis of Free-Surface Flows of Saturated Granular-Liquid Mixtures

D. BERZI[1] AND J.T. JENKINS[2]

[1]Department of Environmental, Hydraulic, Infrastructures and Surveying Engineering, Politecnico di Milano, Milan 20133, Italy

[2]Department of Theoretical and Applied Mechanics, Cornell University, Ithaca, NY 14853 USA

(Received 13 May 2008)

A simple two-phase model for steady, fully developed flows of particles and water over erodible, inclined beds is developed for situations in which the water and particles have the same depth. The rheology of the particles is based on recent numerical simulations and physical experiments, the rheology of the fluid is based on an eddy viscosity, and the interaction between the particles and the fluid is through drag and buoyancy. Numerical solutions of the resulting differential equations and boundary conditions provide velocity profiles of the fluid and particles, the concentration profile of the particles, and the depth of the flow at a given angle of inclination of the bed. Simple approximations permit analytical expressions for the flow velocities and the depth of flow to be obtained that agree with the numerical solutions and those measured in experiments.

1. Introduction

Debris flows are mixtures of water and cohesive or cohesionless particles driven down slopes by gravity. They invariably consist of unsteady, non-uniform surges of heterogeneous mixtures, exhibit strong grain-size segregation, and involve non-hydrostatic distributions of fluid pressure (Iverson 1997).

Because of the high solid concentrations that characterize debris flows, direct interactions between particles are common. Consequently, the resistance to motion associated with frictional collisions between the grains must be taken into account in descriptions of such flows.

Models of debris flows as a single-phase fluid exist. They typically employ a non-Newtonian rheology to incorporate the effect of the grain interactions (see Takahashi 1991; Coussot 1994; Chen & Ling 1998; Brufau *et al.* 2000). The rheologies adopted range from rigid-viscous (yield, followed by a linearly viscous shear stress) (Bingham 1922) to collisional (shear and normal stresses quadratic in the shear rate) (Bagnold 1954). More elaborate models (Iverson 1997; Jenkins & Hanes 1998) distinguish between the two phases and assume that they interact through drag and buoyancy.

In recent years, much research has been devoted to the investigation of inter-particle interactions for the case of dry granular flows, both from theoretical and experimental points of view. In particular, recent extensions of kinetic theories (Mills, Tixier & Loggia 1999, 2000; Aranson & Tsimring 2002; Louge 2003; Kumaran 2006; Jenkins 2006, 2007) and numerical and experimental simulations of motions of disks and spheres (Pouliquen 1999; GDR MiDi 2004; da Cruz 2005) furnish some hints about the possibility of using a simple constitutive model for dense flows of dry grains, at least for the case of steady, fully-developed flows.

In experiments, Armanini *et al.* (2005) investigated the steady fully-developed flow of water and plastic cylinders in a rectangular inclined flume. This is an extremely idealized debris flow. However, because of its simplicity, Armanini and co-workers were able to measure the distributions of velocity, concentration and granular temperature of the grains across the flow and to make comparisons with the predictions of kinetic theories. In their experiments, the mixture of water and grains flowed either over a rigid bottom or over an erodible bed. For the flows over an erodible bed, the authors distinguished three cases, depending on whether the height of the flowing grains was equal to the height of the flowing water (saturated debris flow), the height of the flowing grains was less than the height of the flowing water (oversaturated debris flow) or the height of the flowing grains was greater than the height of the flowing water (undersaturated debris flow).

Our goal is to provide a model of steady, fully-developed debris flows over erodible beds that incorporates the essential physics of the process, reproduces the experimental observations of Armanini *et al.* (2005), and is simple enough to give approximate analytical solutions for engineering applications. Because in saturated flows the fluid and particle phases have a common free surface, the boundary conditions there are simpler than for under- and over-saturated flows. Consequently, we focus here on saturated debris flow, and defer the analysis of the more complicated situations.

The mixture of water and cohesionless granular material is treated as a two-phase flow. A very simple but realistic rheology suggested by experiments on dry granular flow is adopted for modelling the resistance in the particle phase. The rheology results from momentum transfered in collisions that involve more than two particles. As the concentration increases, the number of particles involved in simultaneous collisions increases and ephemeral chains of particles begin to dominate the momentum transfer. In the constitutive relation that describes this, there are two parameters: a yield, associated with the minimum angle for which a steady flow is possible; and the coefficient of the rate dependent part, determined by fitting with experiments. However, once determined for a given granular material, the latter remains fixed and does not depend on the characteristics of the flow. Because the experiments indicate that the interstitial fluid does not influence the interaction between the particles, we do not include such a contribution. It has been incorporated in the context of a single-phase model for submarine debris flows by Cassar, Nicolas & Pouliquen (2005). However, in such flows, the particle interactions are far less violent than in debris flows.

The presence of the sidewalls in the rectangular laboratory flume used by Armanini *et al.* (2005) is taken into account in the way suggested by Taberlet *et al.* (2003), through a Coulomb friction term. Indeed, it has been demonstrated that the sidewall resistance is responsible for the development of an erodible bed in the case of steep, dense, dry granular flows (Taberlet *et al.* 2003; Jop, Forterre & Pouliquen 2005). Here, it is assumed that this is also the case for dense granular–liquid mixtures. In the same spirit, a very simple turbulence model based on the mixing length hypothesis is adopted for the momentum transfer in the liquid phase. Finally, as in other two-phase models, it is assumed that the interaction between the liquid and the solid is due only to buoyancy and drag.

In order to obtain an approximate analytical description of the flow, two further assumptions are made that seem reasonable and consistent with the experimental observations: the solid concentration and the difference in the velocities of the phases across the flow are each taken to be constant. These assumptions permit the derivation of analytical expressions for the velocity profiles of the liquid and particle phases, the depth of the flow and the inclination of the free surface as functions of the particle and liquid discharge. They are also the first step in an iterative procedure leading to improved concentration and velocity profiles.

In § 2, the experiments are described. In § 3, the equations governing the motion of the debris flow are presented and the constitutive models and the simplifying assumptions adopted in this work are introduced. In § 4, comparisons with the experiments performed by Armanini *et al.* (2005) and Larcher *et al.* (2007) are made and discussed. Finally, in § 5, some conclusions and suggestions for future improvements of the present theory are drawn.

2. Experiments

The experiments reported on by Armanini *et al.* (2005) and Larcher *et al.* (2007) were carried out in the recirculating flume shown in figure 1 (from Armanini *et al.* 2005). It consisted of a glass-walled open channel fed by an external conveyor belt. In it, they were able to maintain a steady, fully-developed flow in a section of the channel. Armanini *et al.* (2005) controlled the total amount of water and particles in the flume and its angle of inclination. Given the angle of inclination, a steady, fully-developed flow was achieved in a section of the channel after a certain fraction of the particles was deposited in the bed. In this section of the channel, the inclination of the bed was, in general, different from the inclination of the flume. The inclination of the bed then determined the volume flow rates of water and particles above it. In steady, fully-developed conditions, the angle of inclination of the free surface is equal to that of the bed.
The steady, fully-developed debris flow was filmed through the glass wall of the open channel using a high-speed video camera. An example of a single frame is shown in figure 2 (from Armanini *et al.* 2005). It is possible to see the variation of the velocity and solid concentration moving from the free surface towards the bed. Using image processing techniques, Armanini *et al.* (2005) were able to obtain a detailed description of the flow in terms of the distributions of grain velocity, concentration, granular temperature and stresses. These are crucial pieces of information for evaluating the capability of a mathematical model to capture the key features of a debris flow.
The goals of the present work are to predict the depth of the flow and the profiles of grain velocity, water velocity, and concentration, given the angle of inclination of the bed, to calculate the total flux of grains and water from these, and to compare the profiles and the fluxes with those measured in the experiments.

3. Theory

A sketch of the geometry of a saturated debris flow over an erodible bed is shown in figure 3. We take $z = 0$ to be the free surface and $z = h$ the erodible bed, and let ρ denote the fluid mass density, c the grain concentration, g the gravitational acceleration, θ the free surface inclination, σ the grain specific mass, d the grain diameter, η the fluid viscosity, U the fluid velocity, and u the grain velocity.

3.1. *Fluid Momentum Balance*

The balance of fluid momentum transverse to the flow is

$$P' = \rho g \cos\theta, \tag{3.1}$$

where P is the fluid pressure. Here and in the following a prime indicates a derivative with respect to z.
The balance of fluid momentum in the direction of flow is

$$S' = (1 - c)\,\rho g \sin\theta - \Delta, \tag{3.2}$$

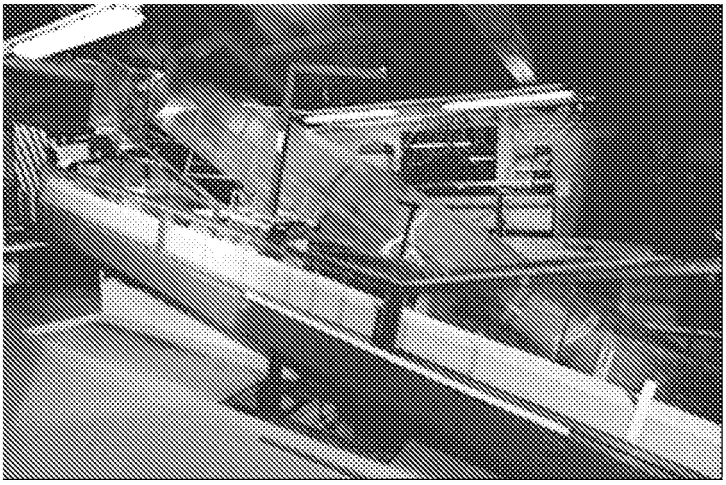

FIGURE 1. The re-circulating flume used by Armanini *et al.* (2005) (published by permission of Cambridge University Press).

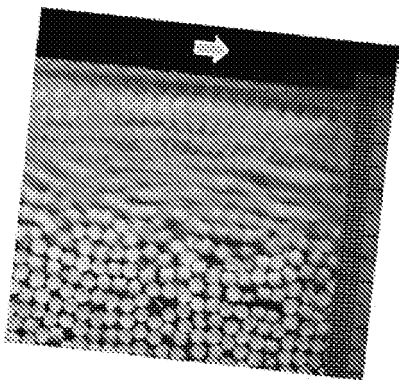

FIGURE 2. A frame of a steady, fully-developed flow (from Armanini *et al.* 2005, published by permission of Cambridge University Press).

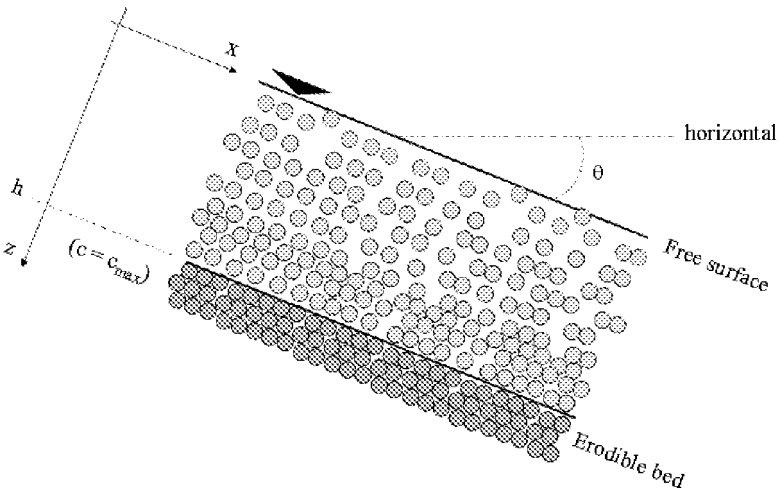

FIGURE 3. Sketch of a saturated debris flow over an erodible bed.

where

$$S = -(1-c)\left[\rho\kappa^2(h-z)^2 \mid U' \mid\right] U' \tag{3.3}$$

is the fluid shear stress and

$$\Delta = \rho\frac{c}{d}\frac{1}{(1-c)^{3.1}}\left(\frac{3}{10} \mid U-u \mid +18.3\frac{\eta}{\rho d}\right)(U-u) \tag{3.4}$$

is the drag. In the constitutive relation (3.3) for the fluid shear stress, the approximation is made that the mixing length in the turbulent viscosity is proportional to the distance from the bed through Karman's constant, $\kappa = 0.41$. The presence of the particles is expected to influence the turbulence, but in the absence of any data, we have no information to guide a modification of this parameter. In order to avoid the logarithmic singularity in the velocity profile, we replace the turbulent viscosity with the molecular viscosity very close to the bed, where the latter exceeds the former. The expression (3.4) for the drag is, perhaps, the simplest form of a drag force (Dallavalle 1943) that incorporates viscous drag, form drag, and concentration dependence (Richardson & Zaki 1954).

3.2. *Particle Momentum Balance*

The balance of particle momentum transverse to the flow is

$$p' = \rho c\,(\sigma - 1)\,g\cos\theta, \tag{3.5}$$

where p is the particle pressure. Here, buoyancy has been incorporated in the dimensionless body force. If W is the chute width and μ_w the wall friction, the corresponding component parallel to the flow is

$$s' = \rho\sigma c g\sin\theta + \Delta - 2\frac{\mu_w}{W}p, \tag{3.6}$$

where s is the grain shear stress. Here, it is assumed that the sidewalls exert a frictional force on the particles, as in the case of dry granular flow (Taberlet *et al.* 2003; Jop *et al.* 2005). The use of this term in the particle momentum balance implies an influence of the channel width on the particle transport capacity. However, in interpreting their experimental results, Armanini *et al.* (2005) did not regard the influence of the sidewalls as being significant. The importance of the sidewall friction will be evaluated in the context of an approximate analytic solution for the velocity profiles.

In the version of the GDR MiDi (2004) rheology that we employ, the grain shear stress is given in terms of p and an effective coefficient of friction μ:

$$s = \mu p. \tag{3.7}$$

Dimensional analysis shows that for one-dimensional shearing flows that are homogeneous and steady, μ and c are only functions of the inertial parameter

$$I = \frac{d \mid u' \mid}{(p/\rho c\sigma)^{1/2}}. \tag{3.8}$$

The inertial parameter is the ratio of time scales associated with grain motion perpendicular and parallel to the flow, respectively. Cassar *et al.* (2005) suggest that the definition (3.8) of the inertial parameter is valid only in the free fall regime identified by Courrech du Pont *et al.* (2003), in which the particle inertia dominates the fluid drag. This is the case in the experiments on saturated debris flow performed by Armanini *et al.* (2005).

The flow behaviour results from momentum transferred in collisions that involve more than two particles. As the concentration increases, the number of particles involved in

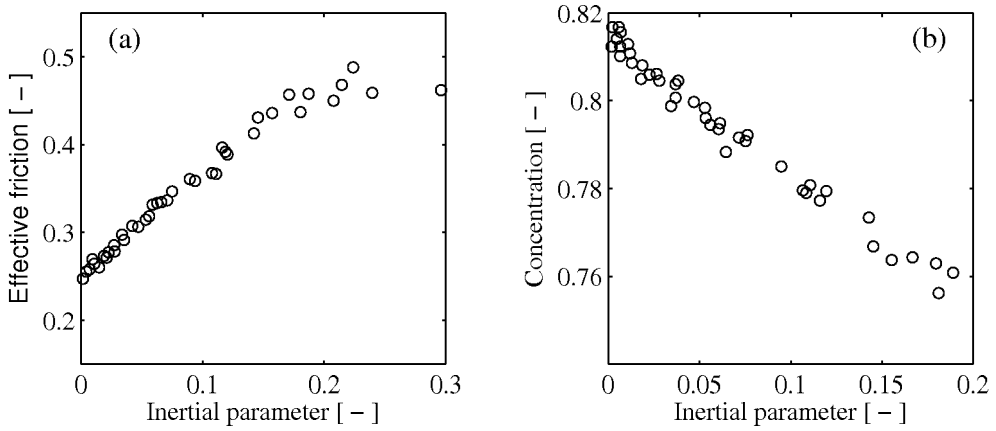

FIGURE 4. (a) The linear relation between effective friction μ and inertial parameter I for circular disks (from da Cruz *et al.* 2005). (b) The corresponding linear relation between concentration and I.

simultaneous collisions increases and ephemeral chains of particles begin to dominate the momentum transfer. This is responsible for a smooth transition from a regime that involves multiple, simultaneous collisions to a regime that involve static chains of contacting particles in the bed.

The algebraic relation between the stress ratio and the inertial parameter can be placed in the context of the kinetic theory and a slight extension of it appropriate to dense flows. When the divergence of the flux of fluctuation energy of the kinetic theory vanishes, an algebraic determination of the granular temperature in terms of the shear rate is possible. Numerical simulations of dense, dry flows (Silbert *et al.* 2001; Mitarai & Nakanishi 2005) indicate that this is the case in dense flows over an inclined, rigid bed in the absence of sidewalls. Then, as indicated by Jenkins (2006) a correspondence can be made between the rheology that involves the inertial parameter and that of the kinetic theory, at least in the region of the flow in which collisions dominate the particle interactions.

Numerical experiments on simple shear flows of disks (figures 4a,b from da Cruz *et al.* 2005) suggest that at high solid concentrations simple linear expressions are valid for μ:

$$\mu = \mu_{min} + \chi I, \tag{3.9}$$

and c

$$c = c_{max} - bI, \tag{3.10}$$

where μ_{min}, χ, c_{max} and b are numerical coefficients. The coefficient μ_{min} is the smallest value of μ for a steady, fully-developed flow and c_{max} is the corresponding value of the particle concentration.

Figure 4a suggests that the effective friction saturates at large values of the inertial parameter (GDR MiDi 2004; Jop *et al.* 2005). This saturation has been related to the existence of a maximum angle for steady, fully-developed, dry granular flows over an inclined plane (Pouliquen 1999). Saturation can be incorporated in the simple rheology by assuming that (3.9) is valid up to a maximum value μ_{max} of the effective friction and constant thereafter.

3.3. *Boundary Conditions*

In order to solve the flow problem, we need to specify boundary conditions. At the common free surface of the particles and water, we assume that the stresses vanish

$$P\,(0) = 0,\ S\,(0) = 0,\ p\,(0) = 0 \text{ and } s\,(0) = 0. \tag{3.11}$$

When dealing with granular flows over an erodible bed, it is necessary to determine the location of the bed. This requires that the physical characteristics of the bed be specified. Experiments on inclined dry particle flows carried out over extremely long times indicate that the bed creeps (Komatsu *et al.* 2001). However, over the much shorter time scales of the experiments performed by Armanini *et al.* (2005), it is reasonable to assume that the grains in the bed remain fixed, so that

$$u(h) = 0. \tag{3.12}$$

This implies that in the bed the effective friction has a value less than or equal to μ_{min} and the concentration is greater than or equal to c_{max}, where the equalities apply at the interface with the flowing layer:

$$s(h)/p(h) = \mu_{min} \text{ and } c(h) = c_{max}. \tag{3.13}$$

A final assumption is that the fluid shear stress vanishes in the bed, so that the gravitational force is balanced only by the drag force. The study of dense collisional flows of massive sediment by Jenkins and Hanes (1998) indicates that the shear stress in the fluid phase is essentially zero at the bed and the total shear stress there is dominated by momentum transferred in particle interactions. Then, as in groundwater flows (de Marsily 1981),

$$(1 - c_{max})\sin\theta - c_{max}C\,|_{z=h}\,U(h) = 0, \tag{3.14}$$

where

$$C\,|_{z=h} = \frac{1}{(1 - c_{max})^{3.1}}\left[\frac{3}{10}U(h) + 18.3\frac{\eta}{\rho d}\right]. \tag{3.15}$$

3.4. *Numerical Solution*

In order to obtain numerical solutions, the momentum balances and constitutive relations are phrased in terms of dimensionless variables, with lengths made dimensionless by d, velocities by $(gd)^{1/2}$, and stresses by $\rho\sigma gd$. For simplicity, in the following, the notation already introduced for the dimensional variables will be employed for their dimensionless counterparts. The resulting system of six first order ordinary differential equations for P, S, U, p, s and u on the interval $0 \leqslant z \leqslant h$ are, then,

$$P' = \frac{1}{\sigma}\cos\theta; \tag{3.16}$$

$$S' = (1 - c)\frac{1}{\sigma}\sin\theta - \frac{c}{\sigma}C(U - u), \tag{3.17}$$

where

$$C = \frac{1}{(1 - c)^{3.1}}\left(\frac{3}{10}\mid U - u \mid + \frac{18.3}{\mathrm{R}}\right), \tag{3.18}$$

with $\mathrm{R} = \rho d(gd)^{1/2}/\eta$;

$$U' = -\left[\frac{\sigma S}{(1 - c)\kappa^2(h - z)^2}\right]^{1/2}, \tag{3.19}$$

where this is regularized by the molecular viscosity at the bed;

$$p' = \left(1 - \frac{1}{\sigma}\right) c \cos\theta; \tag{3.20}$$

$$s' = c \sin\theta + \frac{1}{\sigma} cC(U-u) - 2\frac{\mu_w}{W} p; \tag{3.21}$$

$$u' = -\left(\frac{p}{c}\right)^{1/2} \frac{c_{max} - c}{b}, \tag{3.22}$$

where

$$c = c_{max} - \frac{b}{\chi}\left(\frac{s}{p} - \mu_{min}\right). \tag{3.23}$$

At the free surface, the indeterminate form $s/p = 0/0$ is evaluated using L'Hospital's rule:

$$\left.\frac{s}{p}\right|_{z=0} = \lim_{z\to 0} \frac{s'}{p'} = \frac{\sigma}{\sigma - 1} \tan\theta + \frac{1}{\sigma - 1} \left.\frac{C(U-u)}{\cos\theta}\right|_{z=0}. \tag{3.24}$$

The seven boundary conditions associated with the system of first order equations are:

$$P(0) = 0,\ p(0) = 0,\ S(0) = 0,\ s(0) = 0,\ u(h) = 0,\ s(h) - \mu_{min} p(h) = 0, \tag{3.25}$$

and

$$(1 - c_{max}) \sin\theta - c_{max} C\,|_{z=h}\, U(h) = 0. \tag{3.26}$$

The additional boundary condition permits the determination of the depth h as part of the solution.

In a numerical solution, the angle of inclination is specified and the MATLAB© program bvp4c is employed to predict $P(z)$, $S(z)$, $U(z)$, $p(z)$, $s(z)$, $u(z)$, and h. From these, the concentration $c(z)$ can be evaluated. Then, the volume fluxes of grains q and of fluid Q may be calculated using

$$q = W \int_0^h c(z) u(z) \mathrm{d}z \text{ and } Q = W \int_0^h [1 - c(z)]\, u(z) \mathrm{d}z. \tag{3.27}$$

In the next sub-section, the results of such a numerical solution are compared with those of a simple analytical approximation.

3.5. *Approximate Analytical Solution*

To obtain approximate analytical solutions, three approximations are made:

i) in the turbulent viscosity, the mixing length is assumed to be constant and the turbulent viscosity is taken to be its average through the flow,

$$S = \frac{1}{\sigma}(1 - c) k^2 h^2 U'^2, \tag{3.28}$$

where $k = 0.20$; ii) the concentration is initially assumed to be constant

$$c = \bar{c}\ ; \text{ and} \tag{3.29}$$

iii) because the densities of the particles and fluid are not so different, the particle and fluid velocity profiles are assumed to have a similar shape; hence,

$$u' = U'. \tag{3.30}$$

That is, the difference between the particle and fluid velocities is assumed to be constant. The drag force (3.4) can be used in the particle flow momentum balance (3.6) and the

resulting equation integrated to obtain the distribution of the particle shear stress. In dimensionless terms this yields

$$s = \sin\theta \int_0^z c\mathrm{d}z + \frac{1}{\sigma}\sin\theta \int_0^z (1-c)\mathrm{d}z - S - 2\frac{\mu_w}{W}\int_0^z p\mathrm{d}z. \tag{3.31}$$

Similarly, the distribution of the particle pressure can be obtained through integration of (3.5). The dimensionless result is

$$p = \cos\theta\left(1-\frac{1}{\sigma}\right)\int_0^z c\mathrm{d}z. \tag{3.32}$$

With the approximation (3.28) for the fluid shear stress, the ratio of particle shear stress and pressure is, from (3.31) and (3.32),

$$\frac{s}{p} = \frac{\sigma}{\sigma-1}\tan\theta + \frac{\int_0^z (1-c)\mathrm{d}z}{(\sigma-1)\int_0^z c\mathrm{d}z}\tan\theta - \frac{(1-c)k^2h^2U'^2}{\sigma p} - 2\frac{\mu_w}{W}\frac{\int_0^z\left(\int_0^\zeta c\mathrm{d}z\right)\mathrm{d}\zeta}{\int_0^z c\mathrm{d}z}. \tag{3.33}$$

With the approximations of constant concentration (3.29) and constant difference in the particle and fluid velocities (3.30), (3.33) may be rewritten as

$$\mu = \frac{\sigma}{\sigma-1}\tan\theta + \frac{1}{\sigma-1}\frac{1-\bar{c}}{\bar{c}}\tan\theta - k^2h^2\frac{1}{\sigma}\frac{1-\bar{c}}{\bar{c}}I^2 - \frac{z}{W}\mu_w, \tag{3.34}$$

where

$$I = -\frac{u'}{(p/\bar{c})^{1/2}} = -\frac{u'}{(1-1/\sigma)z\cos\theta}. \tag{3.35}$$

Equation (3.34) provides an explicit characterization, in the context of the approximations, of how particle gravity, fluid gravity, turbulent shear stress and sidewall friction influence the stress ratio of the particle phase. In the limit $\sigma \to \infty$, (3.34) contains as a special case the dry granular flow over an inclined bed between vertical sidewalls studied by Jop *et al.* (2005) and, in the limit $\sigma \to \infty$ and $W \to \infty$, the dry granular flow over an inclined rigid bed in the experiments of Pouliquen (1999).

In figure 5, the contribution of each of these terms to the total is indicated for the parameters of the model introduced in the next Section, for $\theta = 8.5°$. The buoyancy reduces the particle pressure with respect to the dry case and, therefore, the particle gravity is enough to maintain the motion of the grains at values of the angle of inclination much lower than the angle of repose of the dry material. Indeed, figure 5 shows that the particle gravity is greater than μ_{min}, the value of μ at the bed. The sum of fluid gravity and turbulent shear stress is the drag acting on the particles. The absolute value of the turbulent shear stress is maximum at the free surface, where it is of the same order of magnitude as the fluid gravity. Consequently, the drag there is small and could also change sign, while it has a positive maximum at the bed. This explains why, in the numerical solution introduced later in this sub-Section, the fluid in the lower part of the flow is faster than the particles, corresponding to a a positive drag; while that in the region close to the free surface is slower, corresponding to a negative drag.

In the context of the model, the term associated with the sidewall friction provides the only mechanism, responsible for the development of an erodible bed in a steady, fully-developed flow. Indeed, it permits the stress ratio μ to decrease with distance from the free surface and to reach its minimum value μ_{min} at the bed. Given that the bed is characterized by particles with zero velocity and, at $z = h$, $U' = u' = 0$, $I = 0$ and

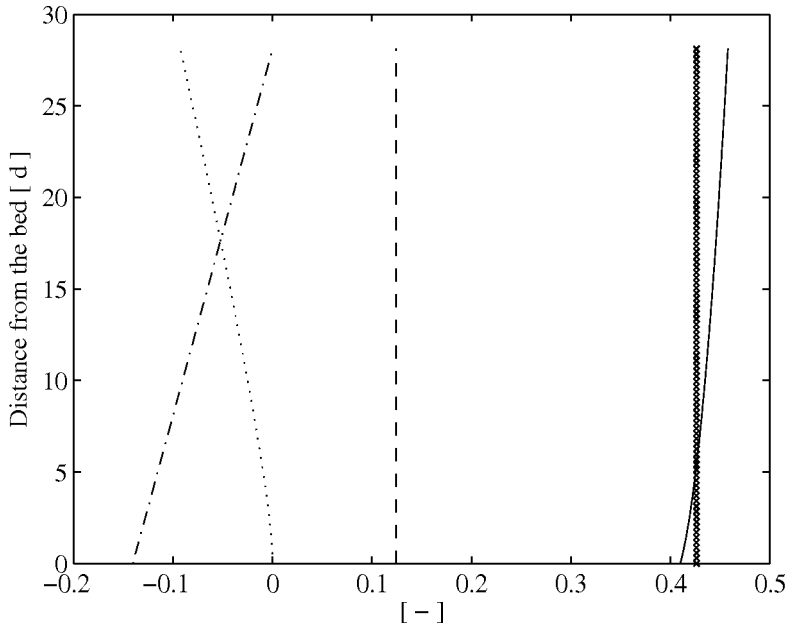

FIGURE 5. Individual contributions to the stress ratio through the depth of the flow: (xxx) particle gravity; (- - -) fluid gravity; ($\cdots$) fluid turbulence; (- $\cdot$ -) sidewalls; (—) total effective friction μ.

$\mu = \mu_{min}$, the depth of the flowing layer can be determined from (3.34):

$$h = \left[\left(1 + \frac{1-\bar{c}}{\bar{c}}\frac{1}{\sigma}\right)\frac{\sigma}{\sigma-1}\frac{\tan\theta}{\mu_w} - \frac{\mu_{min}}{\mu_w}\right] W. \tag{3.36}$$

In addition, (3.34) provides the maximum and minimum angles of inclination for steady, fully-developed flow. Because, at $z = 0$, μ must be greater than μ_{min},

$$\tan\theta \geqslant \frac{\mu_{min}}{1 + (1/\sigma)(1-\bar{c})/\bar{c}}; \tag{3.37}$$

and, because it also must be less than μ_{max} there,

$$\tan\theta \leqslant \left(1 - \frac{1}{\sigma}\right)\frac{\mu_{max} + (k/\chi)^2 h^2 (1/\sigma)(\mu_{max} - \mu_{min})^2(1-\bar{c})/\bar{c}}{1 + (1/\sigma)(1-\bar{c})/\bar{c}}. \tag{3.38}$$

Knowledge of μ_{min} and μ_{max} determines the range of angles for which steady, fully-developed flows are possible. Alternatively, the range of angles for which such flows are possible for a given angle of inclination can be used to determine μ_{min} and μ_{max}.
In (3.37) and (3.38), the rheology $\mu = \mu_{min} + \chi I$ was employed to infer that for $\mu = \mu_{min}$, $I = 0$ and for $\mu = \mu_{max}$, $I = (\mu_{max} - \mu_{min})/\chi$. This rheology is then used in (3.34) to obtain the quadratic equation,

$$\frac{k^2 h^2}{\sigma}\frac{1-\bar{c}}{\bar{c}} I^2 + \chi I - \left[\frac{1}{\sigma-1}\left(\sigma + \frac{1-\bar{c}}{\bar{c}}\right)\tan\theta - \mu_{min} - \frac{z}{W}\mu_w\right] = 0. \tag{3.39}$$

This quadratic may be solved for I and integrated to obtain the particle velocity profile:

$$\frac{u}{(1-1/\sigma)^{1/2}} = -\frac{\chi(\cos\theta)^{1/2}}{3D}\left(h^{3/2} - z^{3/2}\right)$$

$$-\frac{(BD\cos\theta)^{1/2}}{2D}\left[(z-F)\left(2Fz-z^2\right)^{1/2}+F^2\sin^{-1}\left(\frac{z-F}{F}\right)\right]$$
$$+\frac{(BD\cos\theta)^{1/2}}{2D}\left[(h-F)\left(2Fh-h^2\right)^{1/2}+F^2\sin^{-1}\left(\frac{h-F}{F}\right)\right], \tag{3.40}$$

where

$$A=\frac{\tan\theta}{\sigma-1}\left(\sigma+\frac{1-\bar{c}}{\bar{c}}\right)-\mu_{min},\ B=\frac{\mu_w}{W},\ D=k^2h^2\frac{1}{\sigma}\frac{1-\bar{c}}{\bar{c}},\ \text{and}\ F=\frac{\chi^2+4AD}{8BD}. \tag{3.41}$$

The constant difference between the fluid and particle velocities can be determined by solving the quadratic equation

$$(U-u)^2+\frac{18.3}{0.3R}(U-u)-\frac{(1-c_{max})^{4.1}}{0.3c_{max}}\sin\theta=0 \tag{3.42}$$

that results from the boundary condition (3.14).
The analytical expression for the depth-averaged particle velocity can then be obtained by integrating (3.40):

$$\frac{u_m}{(1-1/\sigma)^{1/2}}=-\frac{\chi(\cos\theta)^{1/2}}{5D}h^{3/2}$$
$$+\frac{(BD\cos\theta)^{1/2}}{2D}\left[(h-F)\left(2Fh-h^2\right)^{1/2}+F^2\sin^{-1}\left(\frac{h-F}{F}\right)\right]$$
$$-\frac{(BD\cos\theta)^{1/2}}{2hD}\left\{-\frac{\left(2Fh-h^2\right)^{3/2}}{3}+F^3\left[\frac{h-F}{F}\sin^{-1}\left(\frac{h-F}{F}\right)\right.\right.$$
$$\left.\left.+\sqrt{1-\left(\frac{h-F}{F}\right)^2}-\frac{\pi}{2}\right]\right\}. \tag{3.43}$$

The volume flux of particles associated with this is simply

$$q=\bar{c}u_mhW. \tag{3.44}$$

In the following, the analytical and the numerical solutions are compared for the parameters of the model that are introduced in the next Section; in particular, $\chi=0.5$, $\mu_w=0.27$ and $\mu_{min}=0.41$. For simplicity, the concentration is taken to be $\bar{c}=c_{max}$. The assumption of a constant concentration $\bar{c}$ in the flow is the first step in an iterative process. Indeed, once the distribution of the inertial parameter is obtained by solving (3.39), it is possible to evaluate the analytical distribution of the concentration using the linear rheology of (3.10). For this and for the numerical solution, the parameter b of the rheology is required. The numerical simulations of da Cruz *et al.* (2005) on disks and Mitarai & Nakanishi (2007) on spheres show that the ratio b/χ is in the range 0.4 to 0.8. Here, in order to evaluate the sensitivity of the solutions to this parameter, we take b equal to 0.05 and 0.50, corresponding to ratios b/χ equal, respectively, to 0.1 and 1.
In figure 6, the fluid and particle velocity distributions obtained from the numerical solution of (3.16)-(3.23) are compared with the profiles of the analytical solution. First, the difference between fluid and grain velocities is small both for the analytical and the numerical solution. Figure 5 shows that this is due to a large drag coefficient and not to a negligible drag force, which is of the same order of magnitude as the other terms in (3.34). The figure also indicates that the solution is not very sensitive to the parameter

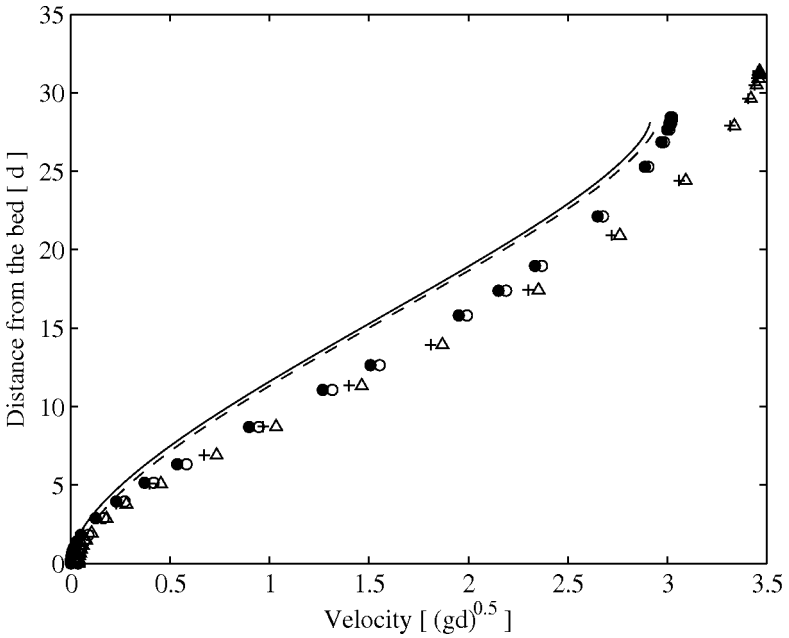

FIGURE 6. Comparison between analytical and numerical velocity distributions: (—) analytical grain velocity; (- - -) analytical fluid velocity; (•) numerical grain velocity and (∘) numerical fluid velocity when $b = 0.05$; (+) numerical grain velocity and (△) numerical fluid velocity when $b = 0.50$.

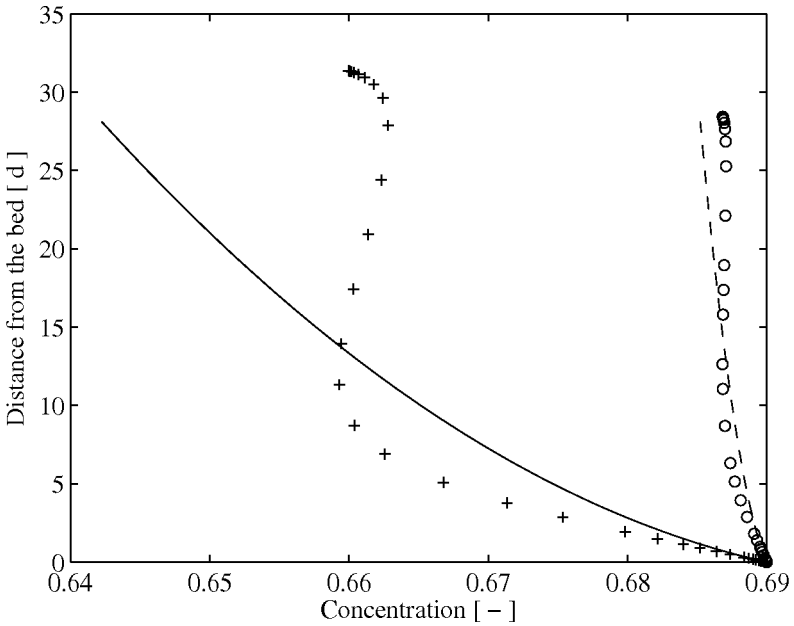

FIGURE 7. Comparison between analytical and numerical distributions of the particle concentration: (—) analytical and (+) numerical concentration profiles when $b = 0.50$; (- - -) analytical and (∘) numerical concentration profiles when $b = 0.05$.

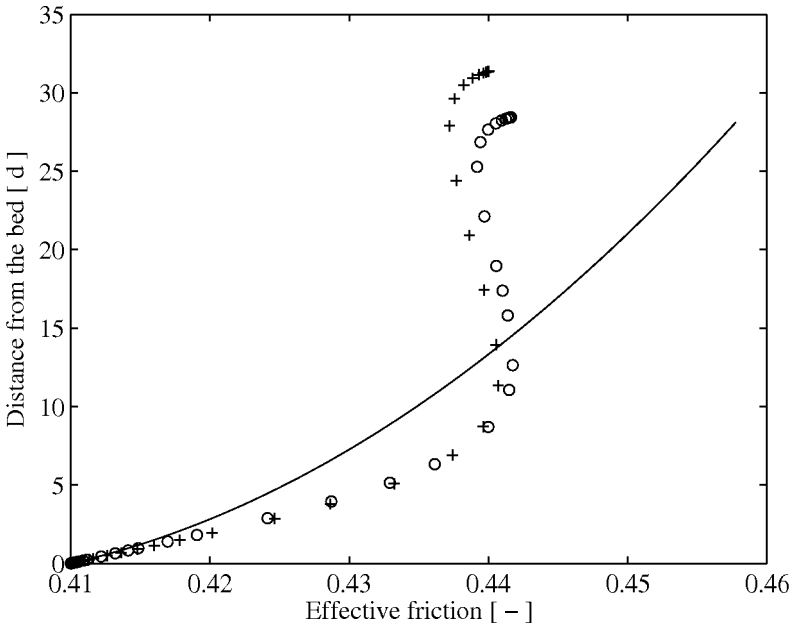

FIGURE 8. Comparison between analytical and numerical distributions of the effective friction μ: (—) analytical μ-distibution; (+) numerical μ-distribution when $b = 0.50$; (∘) numerical μ-distribution when $b = 0.05$.

b, because its variation by one order of magnitude causes only a slight change in the velocity distribution close to the free surface. Figure 7 shows the comparison between the numerical and the iterated analytical concentration profiles. Apart from the fact that the numerical concentration profiles are S-shaped, while the analytical ones are parabolic, the values of the concentration through the flow are everywhere very close to c_{max}, when $b = 0.05$, and slightly less than c_{max}, when $b = 0.50$.

At first sight, figure 7 seems in contrast with the experimental concentration profiles reported by Armanini *et al.* (2005), which range between 0.30 and 0.69. However, the concentration measurements of Armanini *et al.* (2005) involve great uncertainty when the concentration is high; this is everywhere in the flow except in a thin layer close to the free surface. However, a concentration profile obtained by Spinewine *et al.* (2003) using a more sophisticated stereo imaging system indicates that the concentration may be below 0.50 in as much as the upper third of a saturated flow. At concentrations below 0.50, the divergence of the flux of fluctuation energy is not negligible, the algebraic relation between the stress ratio and the inertial parameter begins to break down, and the simple theory fails to reproduce the distribution of particle concentration.

The difference between analytical and numerical concentration profiles is essentially due to the assumption that $U' = u'$. Indeed, as already mentioned, the numerical solutions show that there is a part of the flow near the top where the grains are faster than the fluid. Consequently, in this part, U' is greater than u', so that the term related to the fluid shear stress in (3.34) is actually greater and the value of μ is less in the numerical solution than in the analytical approximation. The opposite applies to the lower part of the flow. The comparison between analytical and numerical distributions of μ is shown in figure 8.

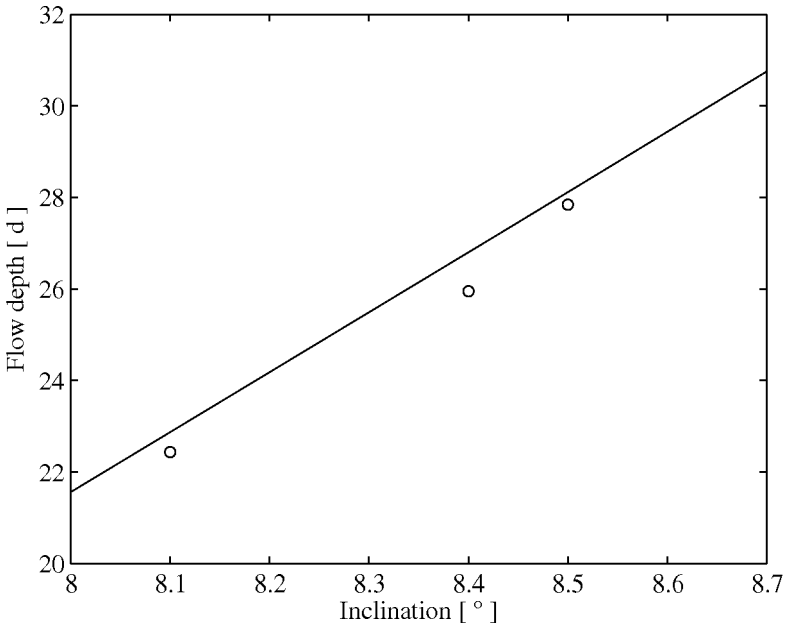

FIGURE 9. Predicted flow depth versus angle of inclination (solid line) and the measured values for the saturated flow (open circles) obtained from Larcher *et al.* (2007).

These defects of the approximate analytical solution and the unavoidable presence of the parameters in the rheology that must be obtained through comparisons with experiments seem small compared to the advantages of dealing with relatively simple and explicit expressions that provide a full description of the flow. We next test the capability of the approximate analytical solution to reproduce the experimental data.

4. Comparison

Here, the predictions of the analytical approximation of the present theory are compared with the measurements of Armanini *et al.* (2005) and Larcher *et al.* (2007). To do this, the parameters measured or suggested by them are adopted. These are $\sigma = 1.54$, $d = 0.0037$ m, $c_{max} = 0.69$ and $W = 54d$. The values of χ and μ_{min} for the rheology and of μ_w for the sidewall friction must be set through fitting with the experiments. Equation (3.36) indicates a linear relation between the flow depth h and the tangent of the bed inclination, $\tan\theta$, where the angular coefficient is proportional to $1/\mu_w$ and the intercept is proportional to μ_{min}/μ_w. Hence, it could be possible to use the experimental values of h against $\tan\theta$ reported by Armanini *et al.* (2005) to evaluate μ_{min} and μ_w. However, Armanini *et al.* (2005) evaluated the flow depth and the mean velocity through depth-averaged momentum and kinetic energy. In conjunction with their definition of the bed, this leads to a value of the grain velocity there that is still one-quarter of its maximum (see their figure 16). To be consistent with our definition of the bed as the place where the grain velocity and the inertial parameter are zero, we have reconsidered the data of Larcher *et al.* (2007) for their saturated flows, and the flow depth has been evaluated as the distance from the free surface where the granular temperature vanishes. Figure 9 shows the experimental values of h versus θ and the theoretical curve of (3.36) with

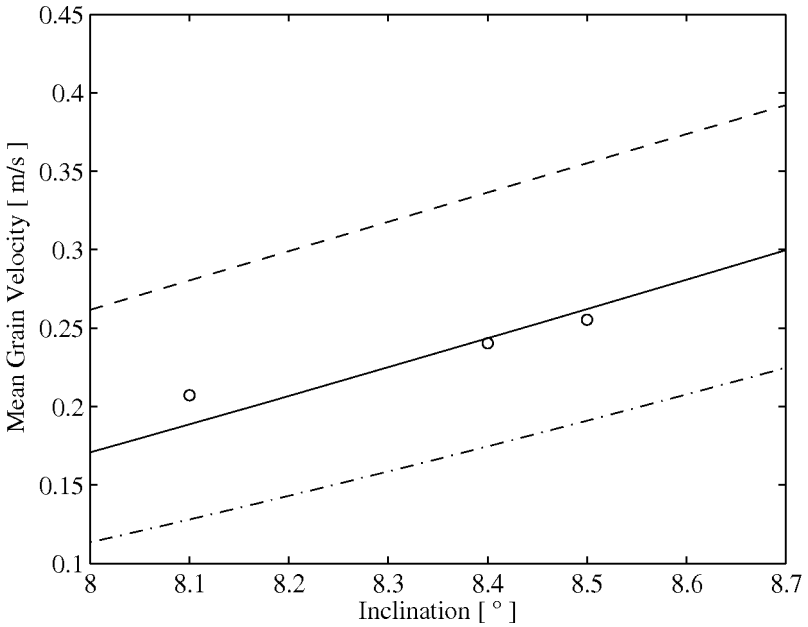

FIGURE 10. Predicted (lines) mean grain velocity versus angle of inclination and the measured (open circles) values for the saturated flow obtained from Larcher *et al.* (2007): (- - -) $\chi = 0.1$; (—) $\chi = 0.5$; (- · -) $\chi = 1.0$.

$\mu_{min} = 0.41$ and $\mu_w = 0.27$. The values of these parameters are close to others reported in literature (Taberlet *et al.* 2003; GDR MiDi 2004; da Cruz *et al.* 2005; Jop *et al.* 2005). The value of χ in the grain rheology has been set through fitting the experimental values of the mean grain velocity obtained from the integration of the velocity profile reported in Larcher *et al.* (2007) over our flow depths. Figure 10 shows that the best fit is obtained for $\chi = 0.5$. The sensitivity of the analytical solution to this parameter is also shown. Decreasing χ by one order of magnitude increases the mean velocity by a factor of two. Figures 11 and 12 show that the parameters determined using global quantities such as depth and mean velocity result in excellent predictions of the distributions of the particle velocities and stresses reported by Larcher *et al.* (2007). Although the small number of experiments does not allow us to truly test the capability of the present theory, the fact that the parameters employed are in good agreement with their corresponding values for dense, dry granular flows provides additional reinforcement for their use.

5. Conclusions

A relatively simple theory based on a realistic rheology for the particle interactions has been applied to steady, fully-developed flows of saturated granular-liquid mixtures over erodible beds. The main aspects of the theory are: (i) the particle rheology is characterized by a linear dependence of the stress ratio on the inertial parameter and by the presence of a yield, as in the case of dense and dry granular flow; (ii) the sidewalls exert on the particles a frictional force, which has been demonstrated to play a fundamental role for dry granular flows over an inclined bed; (iii) the resistance in the interstitial fluid is modelled using a simple turbulent mixing length; (iv) the particle and liquid phases

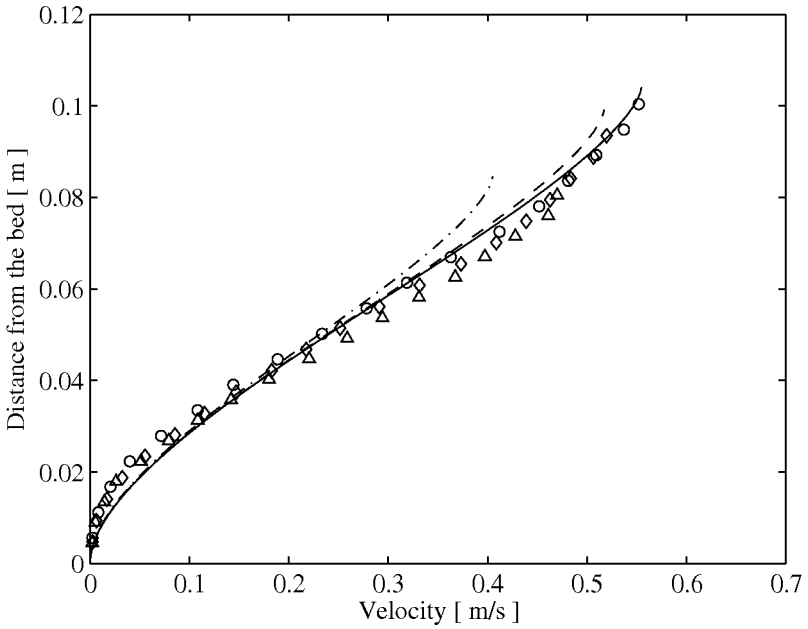

FIGURE 11. Predicted velocity profiles (lines) shown with the measured velocity profiles (symbols, Larcher *et al.* 2007) for the particles: (—) and (∘) for $\theta = 8.5^\circ$; (- - -) and (◇) for $\theta = 8.4^\circ$; (- · -) and (△) for $\theta = 8.1^\circ$.

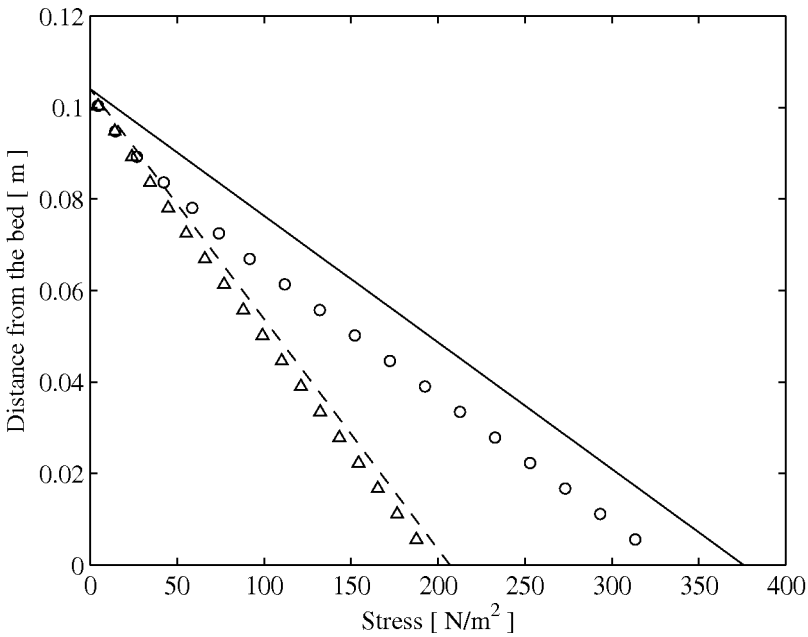

FIGURE 12. Predicted (lines) and measured values (symbols, Larcher *et al.* 2007) of the gravitational contribution to the mixture shear stress (dotted line and open triangles) and of the particle effective normal stress (solid line and open circles) for $\theta = 8.5^\circ$.

interact only through buoyancy and drag. The introduction of three further approximations concerning the constancy of concentration, mixing length and difference between fluid and particle velocities in the flow permits analytical expressions to be obtained for the depth, distributions of fluid and particle velocity, and volume fluxes over a range of free surface inclinations. Such results can be very useful in engineering applications. Three parameters in the model have to be specified through fitting with experiments, but it should be emphasized that at least two of them, the stress ratio for the yield of the bed and the sidewall friction coefficient, have a clear physical meaning, and reasonable values for all of them appear in previous works.

The analytical solutions were tested against the experimental measurements of saturated debris flows made by Armanini *et al.* (2005) and by Larcher *et al.* (2007) in a recirculating flume. The comparisons show that the theory has the capability of reproducing the experimental results. The theory will be extend to include the cases of oversaturated and undersaturated debris flows; that is, when a difference between the depths of the flowing particles and the flowing liquid is present. Steady, fully-developed descriptions of the rheology, similar to those developed here, are often employed in depth averaged descriptions of unsteady, developing flows (e.g. Savage & Hutter 1989; Iverson 1997).

The authors are grateful to Prof. Enrico Larcan for making possible their collaboration and for his support of this study.

REFERENCES

Aranson, I.S. & Tsimring, L.S. 2002 Continuum description of partially fluidized granular flows. *Phys. Rev. E* **65**, 061303.

Armanini, A., Capart, H., Fraccarollo, L. & Larcher, M. 2005 Rheological stratification in experimental free-surface flows of granular-liquid mixtures. *J. Fluid Mech.* **532**, 269–319.

Bagnold, R.A. 1954 Experiments on a gravity-free dispersion of large solid spheres in a newtonian fluid under shear. *Proc. R. Soc. London A* **225**, 49–63.

Bingham, E.C. 1922 *Fluidity and Plasticity*. McGraw-Hill.

Brufau, P., Garcia-Navarro, P., Ghilardi, P., Natale, L. & Savi, F. 2000 1-d mathematical modelling of debris flow. *J. Hyd. Res.* **38** (6), 435–446.

Cassar, C., Nicolas, M. & Pouliquen, O. 2005 Submarine granular flows down inclined planes. *Phys. Fluids* **17**, 103301.

Chen, C.L. & Ling, C.H. 1998 Rheological equations in asymptotic regimes of granular flow. *J. Engrg. Mech.* **124** (3), 301–310.

Coussot, P. 1994 Steady, laminar flow of concentrated mud suspensions in open channel. *J. Hyd. Res.* **32** (4), 535–559.

da Cruz, F., Sacha, E., Prochnow, M., Roux, J. & Chevoir, F. 2005 Rheophysics of dense granular materials : Discrete simulation of plane shear flows. *Phys. Rev. E* **72**, 021309.

Dallavalle, J. 1943 *Micromeritics*. Pitman.

GDR MiDi 2004 On dense granular flows. *Eur. Phys. J. E* **14**, 341–365.

Iverson, R. M. 1997 The physics of debris flows. *Rev. of Geophysics* **35** (3), 245–296.

Jenkins, J.T. 2006 Dense shearing flows of inelastic disks. *Phys. Fluids* **18**, 103307.

Jenkins, J.T. 2007 Dense inclined flows of inelastic spheres. *Gran. Matter* **10**, 47–52.

Jenkins, J.T. & Hanes, D.M. 1998 Collisional sheet flows of sediment driven by a turbulent fluid. *J. Fluid Mech.* **370**, 29–52.

Jop, P., Forterre, Y. & Pouliquen, O. 2005 Crucial role of sidewalls in granular surface flows: consequences for the rheology. *J. Fluid Mech.* **541**, 167–192.

Komatsu, T.S., Inagaki, S., Nakagawa, N. & Nasuno, S. 2001 Creep motion in a granular pile exhibiting steady surface flow. *Phys. Rev. Lett.* **86**, 1757–1760.

Kumaran, V. 2006 The constitutive relation for the granular flow of rough particles and its application to the flow down an incline plane. *J Fluid Mech.* **561**, 1–42.

Larcher, M., Fraccarollo, L., Armanini, A. & Capart, H. 2007 Set of measurement data from flume experiments on steady, uniform debris flows. *J. Hydr. Res.* **45** (extra).

Louge, M.Y. 2003 Model for dense granular flows down bumpy inclines. *Phys. Rev. E* **67**, 061303.

de Marsily, G. 1981 *Quantitative hydrogeology: groundwater hydrology for engineers.* Academic press.

Mills, P., Tixier, M. & Loggia, D. 1999 Model for stationary dense granular flow along an inclined wall. *Europhys. Lett.* **45** (6), 733–738.

Mills, P., Tixier, M. & Loggia, D. 2000 Influence of roughness and dilatancy for dense granular flow along an inclined wall. *Eur. Phys. J. E* **1**, 5–8.

Mitarai, N. & Nakanishi, H. 2005 Bagnold scaling, density plateau, and kinetic theory analysis of dense granular flow. *Phys. Rev. Lett.* **94**, 128001.

Mitarai, N. & Nakanishi, H. 2007 Velocity correlations in dense granular shear flows: Effects on energy dissipation and normal stress. *Phys. Rev. E* **75**, 031305.

Courrech du Pont, S., Gondret, P., Perrin, B. & Rabaud, M. 2003 Granular avalanches in fluids. *Phys. Rev. Lett.* **90**, 044301.

Pouliquen, O. 1999 Scaling laws in granular flows down rough inclined planes. *Phis. Fluids* **11** (3), 542–548.

Richardson, J.F. & Zaki, W.N. 1954 Sedimentation and fluidization. *Trans. Inst. Chem. Engrs.* **32**, 35–53.

Savage, S. B. & Hutter, K. 1989 The motion of a finite mass of granular material down a rough incline. *J. Fluid Mech.* **199**, 177–215.

Silbert, L. E., Ertas, D., Grest, G. S., Halsey, T. C., Levine, D. & Plimpton, S. J. 2001 Granular flow down an inclined plane: Bagnold scaling and rheology. *Phys. Rev. E* **64**, 51302.

Spinewine, B., Capart, H., Larcher, M. & Zech, Y. 2003 Three-dimensional Voronoï imaging methods for the measurement of near-wall particulate flows. *Exp. Fluids* **34**, 227–241.

Taberlet, N., Richard, P., Valance, A., Losert, W., Pasini, J.M., Jenkins, J.T. & Delannay, R. 2003 Superstable granular heap in a thin channel. *Phys. Rev. Lett.* **91**, 264301.

Takahashi, T. 1991 *Debris flow.* IAHR Monograph Series. Balkema.